Delft University of Technology

Scaling DMD modes for modeling Dynamic Induction Control wakes in various wind speeds

Gutknecht, Jonas; Becker, Marcus; Muscari, Claudia; Lutz, Thorsten; Wingerden, Jan Willem Van

Scaling DMD modes for modeling Dynamic Induction Control wakes in various wind speeds

Jonas Gutknecht[1,2,*], Marcus Becker[1], Claudia Muscari[1], Thorsten Lutz[2], Jan-Willem van Wingerden[1]

Abstract— **Dynamic Mode Decomposition (DMD) is a fully data-driven method to extract a linear system from experimental or numerical data. It has proven its suitability for modeling wind turbine wakes, particularly those generated with Dynamic Induction Control (DIC), a method to reduce the wake deficit by enhancing its mixing with the surrounding flow. In this context, DMD may be used to build computationally efficient aerodynamic models suitable for model-based wind farm control algorithms. However, these standard DMD models are only valid for the flow conditions of the training data. This paper presents a novel approach to generalize a DMD model for DIC wakes from the training wind speed to various wind speeds by scaling the DMD modes. For this purpose, we first extract the DMD modes from numerical simulations of a DIC wake at a constant, homogeneous wind speed. Then, we adapt the obtained modes to a different wind speed with a scaling law for the frequency and magnitude derived from the definition of the Strouhal number. This allows for a versatile, efficient application of the DMD model in heterogeneous wind conditions at low computational costs. For validating the presented method, we model a helix wake at 6 ms^{-1} based on the DMD modes from Large Eddy Simulations (LES) at 9 ms^{-1}. The DMD model coincides at a high level with validation simulations, resolving even mid- to small-scale structures.**

I. INTRODUCTION

Complex dynamic systems, such as fluid flows, are in many relevant cases governed by low-dimensional dynamics. These governing dynamics may be extracted by modal decomposition techniques, which assume, that a system's state is a superposition of empirically computed basis vectors, so-called modes. If the system is governed by low-dimensional dynamics, the number of modes necessary to approximate the original state is by magnitudes smaller than the state dimension of the system. These modes are beneficial in two ways: (1) they can give valuable insights into the underlying physical mechanisms of a system, and (2) they can be extrapolated in time to predict a near future state with low computational effort [1].

A modal decomposition technique that inherently features the temporal information about the system is the Dynamic Mode Decomposition (DMD), which was first described by Schmid and Sesterhenn [2]. In contrast to the Proper Orthogonal Decomposition (POD), the standard DMD modes are not orthogonal, but they are associated with a frequency specifying their temporal evolution. Thus, the DMD modes describe the motion of the system from one time instance

to the next, which makes it favorable for predicting a future state. Due to its low computational effort, DMD state prediction is a suitable modeling strategy for model-based control algorithms.

Stemming from the fluid dynamics community, DMD has already proven its benefits in wind energy research: Premaratne and Hu [3] analyzed the wake of a three-bladed wind turbine obtained from particle image velocimetry experiments in a wind tunnel, which was evaluated by numerical experiments from Cherubini et al. [4]. They showed that the near wake is described by one high-frequent mode with a frequency of three times the rotational one, while the far wake contains multiple lower frequent modes.

Besides its huge potential for analyzing a wind turbine wake, DMD has increasingly attracted attention for wake modeling. This is particularly relevant when wind turbines are grouped in wind farms, where some turbines unavoidably operate in the wake of upstream turbines, which can lead to power losses of 35 - 40 %, compared to the standalone case [5] and increased dynamic loads. Veers et al. [6] list the management of the flow through wind farms to enhance power production and reduce maintenance costs as one of the three Grand Challenges that wind energy research needs to address for a successful global energy transition. State prediction with the DMD can contribute to estimating these wake effects and designing wind farm controllers that mitigate them. Iungo et al. [7] developed such a control-oriented, real-time applicable model by training a DMD model on high-fidelity LES simulations of a single wind turbine. Being embedded in a Kalman filter, their model can incorporate live wind speed measurements to achieve an overall model accuracy of $\approx 4\%$.

Annoni et al. [8] present a model of a two-turbine wind farm that processes changes in the pitch angle of the upstream turbine. For this purpose, they apply an advanced version of the DMD that handles problems with forced inputs and outputs, called input-output DMD (IODMD). Cassamo and van Wingerden [9] extend the IODMD with a Koopman Operator to create a model that reproduces the downstream turbines' power dynamics and reconstructs the upstream turbine wake.

In recent years, research has gone beyond just predicting wake losses in wind farms by developing novel control strategies for their mitigation [10]. One promising strategy is Dynamic Induction Control (DIC), which sinusoidally excites the blade pitch signals. Whether this signal is in phase for all the blades or provided with a phase shift provokes a pulsating (later referred to as *pulse*) [11] or a helicoidal (later

[1]Delft Center for Systems and Control, TU Delft, Mekelweg 2, 2628 CD Delft, Netherlands,

[2]University of Stuttgart, Institute for Aerodynamics and Gas Dynamics, Pfaffenwaldring 21, 70569 Stuttgart, Germany

* Corresponding author: J.Gutknecht@tudelft.nl

referred to as *helix*)[12] shape in the wake, respectively. Both enhance the mixing of the wake with the surrounding flow, which results in a faster recovery of the velocity deficit in the wake and, consequently, a higher wind speed at downstream turbines. Frederik et al. [12] observed power gains of up to 7.5% for a two-turbine array when the upstream turbine operates with the helix in numerical studies.

Taschner et al. [13] investigated the helix in a two-turbine array in a conventionally neutral atmospheric boundary layer. Besides significant collective power gains for increasing blade pitch amplitudes, they also identified increased damage equivalent loads on several turbine components. They conclude the necessity for an excitation amplitude that balances both operational parameters. Also in DIC wakes, DMD has already proven its benefits: Muscari et al. [14] analyzed DIC wakes with DMD and found that the most dominant modes fit the excitation frequency of the DIC strategy and its higher integer harmonics.

The application of DIC in a real wind farm requires a wind farm controller, which activates pulse or helix on specific turbines when power gains can be expected. One suitable control strategy is Model Predictive Closed-Loop control, which relies on an aerodynamic model to estimate the wind field in the near future.

The main contribution of this paper is twofold: (1) We present a technique to generalize DMD modes from the training case to cases with changed boundary conditions but the same dimensionless quantities. For this purpose, we derive a scaling law for the frequencies and the shapes of the DMD modes. This addresses a crucial limitation of conventional DMD models, namely that they are only applicable in boundary conditions similar to the training data set. (2) We apply this method to model DIC wakes in cases with equal Strouhal numbers, but different free wind speeds based on one single LES simulation. This results in a versatile and efficient aerodynamic model, oriented to model-based wind farm control algorithms. We test and evaluate this model with an exemplary case of the helix in a non-turbulent regime, which is modeled in a free wind speed of 6 ms^{-1}, based on LES simulations with a free wind speed of 9 ms^{-1}. The remainder of this paper organizes as follows: Section 2 starts with a closer explanation of the DIC and the DMD workflow. It closes with a detailed derivation of the novel DMD mode scaling technique. The simulation setup for the test case is presented in Section 3, followed by an evaluation of the DMD mode scaling technique in Section 4. The paper closes with a conclusion in Section 5.

II. METHODOLOGY

A. Dynamic Induction Control

The blade pitch angles of a wind turbine controlled with DIC are superimposed with sinusoidal signals. These signals are usually characterized by the Strouhal number *St*:

$$St = \frac{f_e D}{u_1}, \tag{1}$$

where f_e denotes the excitation frequency, D the rotor diameter and u_1 the free wind speed. The Strouhal number was identified as a governing parameter for the impact of DIC on the wake. Whether the excitation signal is imposed on the collective pitch angle or the individual pitch angle results in the following two DIC strategies:

1) Pulse: The pulse results from exciting the collective pitch angle with a sinusoid. This leads to an oscillation of the thrust coefficient C_T while the orientation of the thrust remains aligned with the rotational axis. The effects on the wake are significant: the turbine periodically sheds coherent vortex rings that continuously decay on their way downstream. Munters and Meyers [11] optimized these effects with an excitation signal with $St = 0.25$. Even if the pulse has proven to increase the cumulative power of small wind farms, it also increases the power and load fluctuations due to the inherent oscillation of C_T.

2) Helix: The helix, first presented by Frederik et al. [12], achieves recovery effects comparable to the ones achieved with the pulse, but with lower load and power fluctuations. In this case, the individual blade pitch is controlled so that the thrust vector maintains its magnitude. For this purpose, sinusoidal control signals for the tilt and yaw moments with a phase shift $\Delta\phi$ are defined and then transformed to individual blade pitch signals with a Multi-Blade Coordinate Transformation (MBC). As the name suggests, this strategy generates a helicoidal shape in the wake, which rotates depending on the $\Delta\phi$ either twisted in counter-clockwise (CCW) direction ($\Delta\phi = \frac{\pi}{2}$) or in clockwise (CW) direction ($\Delta\phi = \frac{3\pi}{2}$). The CCW helix was found to be more efficient than the CW helix when applied to the upstream turbine of a two-turbine array. With $St = 0.25$ and a blade pitch amplitude of 4 deg, it increases the cumulative power by up to 7.5% compared to a baseline case with both turbines controlled greedily. Additionally, the power and thrust variations are by factor 2 lower than with the pulse.

B. Standard Dynamic Mode Decomposition

The DMD workflow requires a set of m snapshots $\mathbf{x}$ that represent the states of the system at consecutive time instances. The origin of these snapshots is irrelevant. The following description of the DMD workflow is based on [15] and [1].

In the first step, these snapshots $\mathbf{x}$ are arranged into two column matrices $\mathbf{X}$ and $\mathbf{X}'$ in ascending order, such that each column represents the state of the system at one time-step:

$$\mathbf{X} = \begin{bmatrix} \vdots & \vdots & \vdots & & \vdots \\ \mathbf{x}_1 & \mathbf{x}_2 & \mathbf{x}_3 & \cdots & \mathbf{x}_{m-1} \\ \vdots & \vdots & \vdots & & \vdots \end{bmatrix},$$

$$\mathbf{X}' = \begin{bmatrix} \vdots & \vdots & \vdots & & \vdots \\ \mathbf{x}_2 & \mathbf{x}_3 & \mathbf{x}_4 & \cdots & \mathbf{x}_m \\ \vdots & \vdots & \vdots & & \vdots \end{bmatrix} \in \mathbb{R}^{n \times (m-1)}, \tag{2}$$

where n denotes the number of data points per snapshot. $\mathbf{X}'$ can be interpreted as the evolution of $\mathbf{X}$ one time-step

Δt further in time. Then, the DMD aims at finding a linear mapping $\mathbf{A}$ that transfers the states in $\mathbf{X}$ to their subsequent states in $\mathbf{X}'$:

$$\mathbf{X}' = \mathbf{A}\mathbf{X}, \qquad \mathbf{A} \in \mathbb{R}^{n \times n}. \tag{3}$$

The DMD modes consist of a spatial description, defined by the eigenvectors of $\mathbf{A}$, and a temporal evolution, or more specifically, a frequency and a decay rate defined by the corresponding eigenvalues.

The rank of $\mathbf{A}$ is, in most cases, too high to perform the eigendecomposition directly. Consequently, the DMD algorithm circumvents computing $\mathbf{A}$ by considering a rank-reduced representation in terms of a POD-projected matrix $\tilde{\mathbf{A}}$. For this purpose, the first step of the DMD algorithm is to perform a Singular Value Decomposition (SVD) of $\mathbf{X}$:

$$\mathbf{X} \approx \mathbf{U}\Sigma\mathbf{V}^*, \tag{4}$$

where * denotes the conjugate transpose, $\mathbf{U} \in \mathbb{C}^{n \times r}$, $\Sigma \in \mathbb{R}^{r \times r}$ and $\mathbf{V}^* \in \mathbb{C}^{r \times (m-1)}$. $\mathbf{U}$ contains the left singular vectors and Σ the corresponding singular values in descending order on its main diagonal. The truncation order $r < m$ defines the dimension of the POD space and, accordingly, how many singular values are considered in further calculations. Consequently, r governs the number of extracted DMD modes and the level of approximation to the underlying system. A sharp decay of the singular values implies that the system features low-dimensional dynamics and r can be chosen relatively small.

$\tilde{\mathbf{A}}$ is then computed as

$$\tilde{\mathbf{A}} = \mathbf{U}^*\mathbf{A}\mathbf{U} = \mathbf{U}^*\mathbf{X}'\mathbf{V}\Sigma^{-1}, \ \tilde{\mathbf{A}} \in \mathbb{R}^{r \times r}, \tag{5}$$

where $\tilde{\mathbf{A}}$ corresponds to the projection of the full matrix $\mathbf{A}$ onto the POD space. The eigenvalues of $\mathbf{A}$ are now obtained from an eigendecomposition of $\tilde{\mathbf{A}}$:

$$\tilde{\mathbf{A}}\mathbf{W} = \mathbf{W}\Lambda, \tag{6}$$

where the main diagonal of Λ contains the eigenvalues λ and the columns of $\mathbf{W}$ the eigenvectors. The eigenvalues λ already describe the temporal evolution of the DMD Modes in real space. In contrast, $\mathbf{W}$ needs to be projected from the POD space to the real space to obtain the eigenvectors Φ of $\mathbf{A}$:

$$\Phi = \mathbf{X}'V\Sigma^{-1}\mathbf{W}, \Phi \in \mathbb{R}^{n \times r}, \tag{7}$$

so that Φ describes the spatial shape of the DMD modes.

In the case of DIC wakes and a suitable dimension of the DMD subspace r, mode 0 corresponds to the constant mean flow ($Im(\Omega) = 0$). Mode 1 oscillates with the excitation frequency f_e of the pitch and the subsequent modes are harmonics of mode 1. The excitation frequency f_e is governed by the Strouhal number St, which is introduced in (1).

The described approach can be formulated as the following regression problem:

$$\underset{rank(\mathbf{A})=r}{\mathrm{argmin}} \left\| \mathbf{X}' - \mathbf{A}\mathbf{X} \right\|_F. \tag{8}$$

Where $\mathbf{A}$ represents a linear best-fit operator that minimizes the error $\mathbf{X}' - \mathbf{A}\mathbf{X}$ with respect to the Frobenius norm.

C. Conservative DMD

In this work, we use a DMD version that is adapted for conservative systems, such as energy-preserving flows like DIC wakes, presented by Baddoo et al. [16]. In contrast to the standard DMD, the modes obtained with the conservative DMD are orthogonal, so they oscillate with constant amplitudes over time. For this purpose, $\mathbf{A}$ must not change the energy of the system but only redistribute energy between the states. This holds if $\mathbf{A}$ is unitary, such that the optimization problem solved by the DMD can be formulated as:

$$\underset{\mathbf{A}^*\mathbf{A}=\mathbf{I}}{\mathrm{argmin}} \left\| \mathbf{X}' - \mathbf{A}\mathbf{X} \right\|_F. \tag{9}$$

where $\mathbf{I}$ is the identity matrix. This is known as the orthogonal Procrustes problem:

$$\mathbf{A} = \mathbf{U}\mathbf{V}^*, \tag{10}$$

where $\mathbf{U}\Sigma\mathbf{V}^* = \mathbf{Y}\mathbf{X}^*$ is the full singular value decomposition. With slight adaptions, this can be integrated into the DMD workflow, as presented by Baddoo et al. [16]. As the DIC wakes are inherently conservative, the conservative DMD performs better than the standard DMD described in Section II-B. However, the presented DMD mode scaling technique is equally applicable to both versions.

D. Future State Prediction with DMD

The DMD modes allow for predicting a system's future state by extrapolating the dynamics beyond the time covered in the training data. Besides the DMD modes (described by the mode shapes Φ and their temporal evolution Λ), this requires one initial snapshot $\mathbf{x}_1$.

For this purpose, the discrete-time formulation of the eigenvalues λ is reformulated to a continuous-time formulation ω:

$$\omega_k = \frac{ln(\lambda_k)}{\Delta t}. \tag{11}$$

A future state can then be approximated as follows:

$$\mathbf{x}(t) \approx \sum_{k=1}^{r} \phi_k e^{\omega_k t} b_k = \Phi e^{\Omega t} \mathbf{b}, \tag{12}$$

where $\Omega = diag(\omega)$ is a diagonal matrix that carries the time-continuous eigenvalues ω_k. The mode shapes Φ are scaled with the initial amplitudes $\mathbf{b}$. This initial condition is determined with one initial snapshot $\mathbf{x}_1$:

$$\mathbf{b} = \Phi^\dagger \mathbf{x}_1 \tag{13}$$

Since Φ is usually not a square matrix, the Moore-Penrose pseudoinverse, denoted with †, is used. Typically, the calculation of pseudoinverse matrices requires a high computational effort. Hence, multiple state predictions of the same dynamic system, as in the presented dynamic wake models, can significantly be accelerated by calculating $\mathbf{b}$ separately and reusing it for all of the required state predictions.

E. DMD Mode Scaling

To derive the main contribution of this work, the DMD mode scaling method, we first define the following two DIC cases:

1) *Case 1* is the training case, from which the dynamic modes (Φ_1, Ω_1) and the initial amplitudes $\mathbf{b_1}$ have been extracted. The Strouhal number St_1 and the free wind speed $u_{1,1}$ are known.

2) *Case 2* is the case which should be modeled with a free wind speed $u_{1,2} \neq u_{1,1}$. The DIC strategy and the Strouhal number $St_2 = St_1$ are the same as in case 1.

The previously described technique to predict a future state with DMD modes is only valid for constant boundary conditions. Consequently, it fails to predict the states of case 2 without having a specific training data set. This represents a decisive limitation because the DIC wake model must be applicable at any free wind speed without needing wind speed-specific training sets. To circumvent that limitation, we assume that the characteristic dynamics of the DIC wake scale with the free wind speed. Consequently, the dynamic modes from case 1 can be adapted to case 2 without additional training data. For this purpose, the spatial and the temporal characterization of the dynamic modes are scaled separately as follows:

1) Scaling of the Spatial Dynamic Characteristics: The standard DMD workflow already contains a manipulation of the spatial dynamics in (12) and (13). The mode shapes Φ are linearly scaled with the initial amplitudes $\mathbf{b}$ to incorporate the boundary conditions given by the initial snapshot $\mathbf{x}_1$. A variation in the free wind speed represents a change in the boundary conditions. Consequently, the effects on the spatial characterization of the DMD modes can be addressed by scaling the initial amplitudes $\mathbf{b}$ linearly to the new wind speed:

$$\mathbf{b}_2 = \underbrace{\frac{u_{1,2}}{u_{1,1}}}_{s} \cdot \mathbf{b}_1, \tag{14}$$

where the ratio of $u_{1,2}$ and $u_{1,1}$ is considered as scaling factor s. As the scaling is linear, scaling Φ with s would lead to the same result.

2) Scaling of the Temporal Dynamic Characteristics: The fact that case 1 and case 2 feature the same Strouhal number allows us to derive the following scaling of the DIC excitation frequency f_e:

$$St_1 = St_2 \quad \Rightarrow \quad \frac{f_{e,1}D}{u_{1,1}} = \frac{f_{e,2}D}{u_{1,2}} \quad \Rightarrow \quad f_{e,2} = f_{e,1} \cdot s \tag{15}$$

Note that this derivation results in the same scaling factor s as in (14). The relevant DMD modes oscillate with the excitation frequency f_e and its integer multiples. Consequently, the scaling with s is similarly valid for the frequencies of the DMD modes, defined by the imaginary components of Ω:

$$Im(\Omega_2) = s \cdot Im(\Omega_1) \tag{16}$$

After scaling the DMD modes from case 1 with the scaling laws described in (14) and (16), they may be used for predicting a state of case 2 with the standard DMD approach according to (12). Thus, the DMD mode scaling technique promises to capture the dominant effects of changed wind speeds in the DIC wake, with minor modifications of the DMD modes. The DMD workflow itself remains unchanged, so the model complexity and computational effort remain low.

III. DATA GENERATION WITH LES

In this work, the helix wake of one turbine is numerically simulated at two different wind speeds. A first case with a free wind speed of 9 ms^{-1} is used to generate the snapshots to train the DMD model. In the second case, the free wind speed is 6 ms^{-1} and serves as an evaluation for the DMD mode scaling model.

Both cases are simulated with the Computational Fluid Dynamics (CFD) toolbox SOWFA (*Simulator fOr Wind Farm Applications*) [17], extended with the helix controller described by Frederik et al. [12]. SOWFA solves the Navier-Stokes equations with a Large Eddy Simulations (LES) scheme. In this work, the turbine is modeled with the Actuator Line Method (ALM). We use the SOWFA setup from Muscari et al. [14] as presented in Tab. I. The base mesh has a spatial discretization of 50 m in the far field and is refined to 3.125 m in the rotor area. Note that a uniform inflow is chosen and the ground is modeled with a slip wall boundary condition to get the pure helix dynamics without additional complexity introduced by turbulence. The helix controller is switched on after a transient phase of 400 s. The simulation results are decimated in spatial and temporal

TABLE I: Characteristics of the SOWFA Setup

Turbine	DTU 10 MW
D	173.3 m
DIC Strategy	helix
St	0.25
Free wind speed u_1	9 ms^{-1} , 6 ms^{-1}
Turbulence intensity I_0	0 %
Time step Δt	0.2 s
Simulation time t	2000 s
Domain extension $x \times y \times z$	$2500 \times 1000 \times 600$ m^3
Cell size in rotor area	3.125 m

dimensions to reduce the data volume processed in the DMD. Besides discarding the transient run-up phase, only every tenth time-step is considered so that the set of snapshots contains $m = 800$ states with a temporal discretization of 2 s. The spatial dimension is reduced by discarding the coarser outer flow grid cells and considering only one of four grid cells in the rotor domain. This results in a domain size of $1712.5 \times 337.5 \times 300$ m^3 with a cell dimension of 12.5 m, hence each snapshot contains data at 96600 gridpoints.

The simulation results contain the velocity components u, v and w in x, y and z direction, respectively, as well as the pressure p. However, the training-dataset only considers the velocity component u as it is the only parameter needed for power estimations of downstream turbines. Ignoring the other flow dimensions reduces the data volume by 75 % without
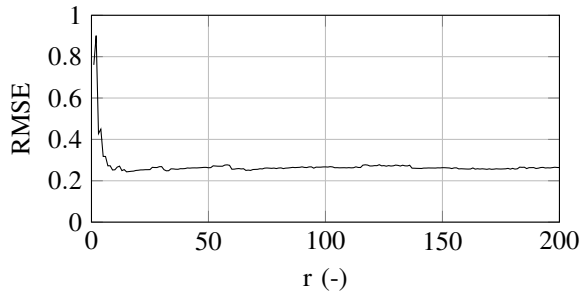
Fig. 1: Influence of the truncation order r on the model accuracy

sacrificing modeling accuracy. The training data contains 800 timesteps, consequently $\mathbf{X}, \mathbf{X}' \in \mathbb{R}^{96600 \times 799}$.

IV. RESULTS

A. Model Evaluation

The truncation order r is the governing parameter of the DMD, as it defines the number of dynamic modes that are extracted and used for the state reconstruction. Consequently, it governs both the computational effort and the model accuracy. Figure 1 determines its influence on the model accuracy by investigating truncation orders $r \in [1, 200]$. Thereby, the results are quantified in terms of the Root Mean Square Error (RMSE), which is calculated based on the element-wise residuals between the true snapshot matrix $\mathbf{X}'$ and its reconstruction $\mathbf{X}'_{DMD,ij}$:

$$RMSE = \sqrt{\frac{1}{nm} \sum_{i=1}^{n} \sum_{j=1}^{m} (\mathbf{X}'_{ij} - \mathbf{X}'_{DMD,ij})^2} \qquad (17)$$

This happens based on the training data set with a free wind speed of 9 ms^{-1}. Note that this formulation averages over all of the contained snapshots meaning that it has no informative value about the temporal evolution of the model accuracy. Figure 1 presents an initial drop of the RMSE for $r \lessapprox 13$ before it converges towards a constant value. This is the typical behavior of a system governed by low-dimensional dynamics [1]. The relevant dynamics can be described with a relatively small number of modes, thus, increasing r does not necessarily improve the accuracy. Consequently, a truncation order of $r = 40$ is chosen as a suitable trade-off between computational efficiency and accuracy.

Table II summarizes the Strouhal numbers of the first five dynamic modes obtained from the training data set.

TABLE II: Strouhal numbers of the dominant DMD modes

Mode	1	2	3	4	5
St_{theory} (-)	0.25	0.5	0.75	1.0	1.25
St_{model} (-)	0.248	0.495	0.743	0.991	1.238
Deviation (%)	0.8	1	0.93	0.9	0.96

As the dynamics excited by the pitch excitation dominate the DIC wake, the modes should be integer harmonics of the excitation Strouhal number $St = 0.25$. The obtained

modes match their theoretical value with minor deviations of ≤ 1 %, which is sufficient for the application in the DMD model. Generally speaking, too-high deviations of the mode frequencies from their theoretical values are expected to decrease the models' scalability significantly.

B. Flowfield Prediction

First, the DMD mode scaling approach is validated qualitatively in its capabilities to model the wake field. For this purpose, Figure 2 visualizes a snapshot of the velocity component u at hub height. The top row shows the SOWFA validation data at 6 ms^{-1}, followed by the modeled wake based on the modes from 9 ms^{-1}. The bottom row presents the local absolute error between the model and the SOWFA simulation.

Before establishing a quasi-steady behavior, the helix requires an undefined run-up phase in SOWFA, which is not captured by the DMD model. Consequently, the modeled wake is not inherently in phase with the validation data but requires a manual alignment. For this purpose, a phase shift is induced and optimized manually to minimize the overall error. Note that this is only required for validation purposes, but not for the application in a real wind farm. The presented snapshots represent the state 400 s after the manual alignment to allow for conclusions on the model accuracy over time. The wake, modeled with the DMD mode scaling method, shows high accordance with the validation simulations. The general shape of the modeled helix is, 400 s after the manual alignment, still in phase with the validation simulations. This indicates, that the suggested DMD mode scaling technique successfully adapts the excitation frequency f_e to the new wind speed. This also results in a suitable manipulation of the advection speed of the characteristic helix flow structure. Within the helix wake, even small- and mid-scale structures with a spatial dimension of 0.25 - 0.5 D are precisely resolved. This is proven by large areas with a low absolute error throughout the entire wake. Only in scattered, isolated areas the absolute error exceeds 1 ms^{-1}. These errors occur primarily in the downstream regions of $x > 5$ D, where a turbulent regime governs the flow. Therefore, we assume the error spots do not relate to the helix dynamics but to stochastic turbulences, which are unfeasible for the DMD. Thus, the evaluation of the flow fields at hub height implies a considerable potential for DMD mode scaling to generalize the DMD modes to various wind speeds. It supports the initial assumption, that a change in the free wind speed doesn't change the dominant dynamic characteristics of the helix fundamentally. They can rather be scaled from the DMD space to the real space with the suggested velocity-dependent scaling laws (14) and (16).

C. Mean Velocity at Virtual Downstream Turbine

Even if the DMD model does so, a highly resolved flow field is not of major importance for the application in an engineering wind farm model. Here, the focus lies on precise estimations of the generated power, which is governed by the wind speed at the rotor plane u_2. In this section, the
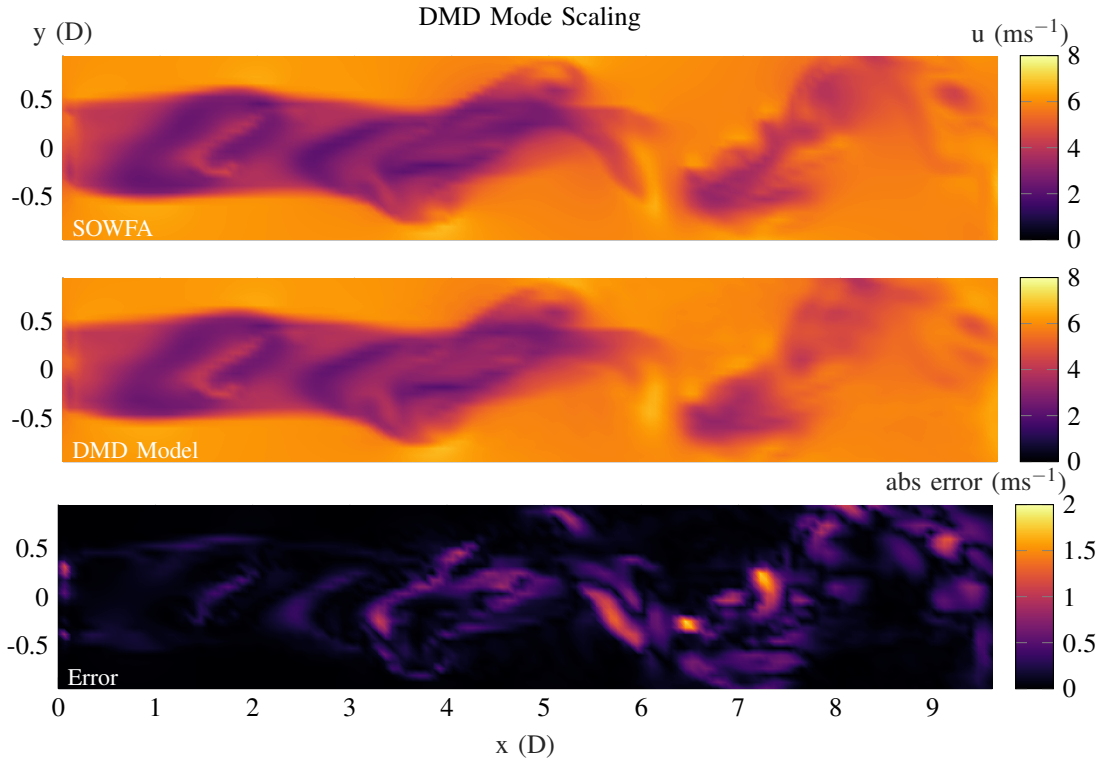
Fig. 2: Comparison of the flow fields at hub height at a free wind speed of 6 ms^{-1}. The SOWFA validation data (top row) is compared to the modeled wake with DMD modes, scaled from 9 ms^{-1} (middle row).

suitability of the DMD mode scaling method for a control-oriented model is evaluated by determining the mean wind speed $\bar{u}_2$ over a circular area $\mathscr{F}$ of diameter D:

$$\bar{u}_2 = \frac{4}{\pi D^2} \iint_{\mathscr{F}} u \, d\sigma, \qquad (18)$$

where $d\sigma$ denotes one surface element. This approach can be considered as placing a virtual turbine in the wake and seeking its effective wind speed. Equation (18) can be evaluated for multiple consecutive time-steps and thus allows for an evaluation of the model accuracy over time.

In this work, multiple virtual turbines are directly aligned with the upstream turbine to evaluate a full wake overlap. Cases with partial wake overlap or yaw misalignment are not considered. Figure 3 compares the temporal evolution of $\bar{u}_2$ at four equidistant virtual downstream turbine positions from the SOWFA validation simulations to the modeled flow.

First, it is noticeable, that the $\bar{u}_2$ amplitudes increase with increasing downstream distance, which is due to the following: The helix wake rotates constantly, consequently, the overlap of the wake core with the virtual turbines varies periodically. In the downstream direction, the crosswind deflection of the helix wake center increases, so the variation of the wake overlap with the virtual turbine does the same. This results in increasing fluctuations of $\bar{u}_2$. Thus, Figure 3 represents reasonable evolutions of $\bar{u}_2$ and can be used for evaluating the DMD model.

As implied by the high accuracy in modeling the flow field at hub height, the modeled temporal evolution of $\bar{u}_2$

coincides in a major part with the SOWFA validation data. Periodicity and magnitude are approximated with a high level of accuracy. Thereby, the period matches the adapted excitation period of $T_e = 118.8$ s, which corresponds to $St = 0.25$ in the given wind speed of 6 ms^{-1}.

It stands out that at $x = 3$ D, the DMD model overestimates $\bar{u}_2$ with a constant offset of ≈ 0.055 ms^{-1}, which corresponds to 0.9% of the free wind speed. The other investigated x-positions do not show such a clear deviation trend. They rather follow the shape of the SOWFA validation data with occasional minor exceptions in the peak areas. It is worth mentioning, that Figure 3 doesn't indicate any tendency to a temporal error growth, which implies that the DMD model is applicable without any run-time limitations.

Overall, Figure 3 suggests that the DMD mode scaling technique is a promising model candidate for predicting the generated power in a wind farm model, as it approximates the mean velocity with a high accuracy independent of run-time and downstream position. Nevertheless, further research is required to evaluate cases with partial wake overlap and to which degree the results from a virtual turbine hold for an actual turbine made of solid material.

D. Computational Efficiency

Apart from the model accuracy, also the computational efficiency is decisive for the applicability of control algorithms. Running on a 12th Gen Intel(R) Core(TM) i7-1265U Processor with 16 GB RAM, the model needs ≈ 0.002 s to estimate one timestep. That value is obtained by averaging
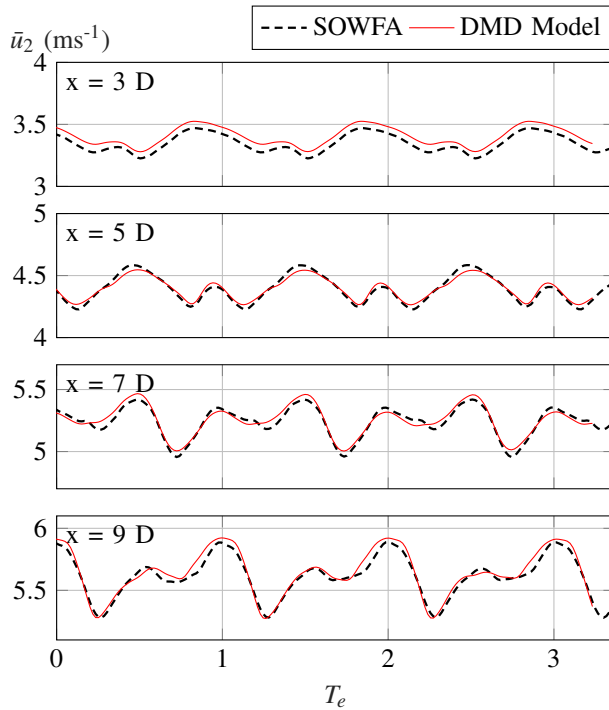
Fig. 3: Validation of the temporal evolution of the mean velocities at downstream virtual turbines at 6 ms^{-1}.

over 5 simulations of 60 timesteps. The time required for data generation and training is not considered, as it has no impact on the computation time in the application phase.

V. CONCLUSIONS AND DISCUSSION

This work presents a method to model dynamic systems in various boundary conditions based on the dynamics of a single training case. In the first step, the dominant dynamics are extracted from the training case with the DMD. Then, a scaling law is presented to adapt the frequency and magnitude of the obtained dynamic modes to changed boundary conditions. The scaled modes can then approximate the state of the system in changed boundary conditions with the standard DMD state reconstruction workflow.

The method is derived and tested with the dynamics of a DIC wake of a wind turbine at various wind speeds. Thereby, the Strouhal number is kept equal in all the cases. It is shown that the method allows for an accurate reconstruction of the helix wake at 6 ms^{-1}, based on the dynamic modes extracted from LES simulations at 9 ms^{-1}, resolving even mid- to small-scale structures. Besides that, the DMD model approximates the mean wind speed $\bar{u}_2$ at virtual turbines placed at multiple downstream positions with a high accuracy. Thus, the DMD mode scaling method represents a promising candidate for a control-oriented aerodynamic DIC wake model to predict a wind farm's power output with low computational effort.

Further research is required to determine the applicability of the presented method in turbulent flow regimes and different free wind speeds.

REFERENCES

[1] J. H. Tu, C. W. Rowley, D. M. Luchtenburg, S. L. Brunton, and J. N. Kutz, "On Dynamic Mode Decomposition: Theory and Applications," *Journal of Computational Dynamics*, vol. 1, no. 2, pp. 391–421, 2014.

[2] P. Schmid and J. Sesterhenn, "Decomposition mode decomposition of numerical and experimental data," *Bull.Amer.Phys.Soc*, 2008, san Antonio/TX.

[3] P. Premaratne and H. Hu, *Analysis of Turbine Wake Characteristics by using Dynamic Mode Decomposition Method*, 2017.

[4] S. Cherubini, G. De Cillis, O. Semeraro, S. Leonardi, and P. De Palma, "Data driven modal decomposition of the wake behind an nrel-5mw wind turbine," *International Journal of Turbomachinery, Propulsion and Power*, vol. 6, no. 4, 2021.

[5] R. Barthelmie, S. Pryor, S. Frandsen, K. S. Hansen, J. Schepers, K. Rados, W. Schlez, A. Neubert, L. Jensen, and S. Neckelmann, "Quantifying the impact of wind turbine wakes on power output at offshore wind farms," *Journal of Atmospheric and Oceanic Technology - J ATMOS OCEAN TECHNOL*, vol. 27, pp. 1302–1317, 08 2010.

[6] P. Veers, K. Dykes, S. Basu, A. Bianchini, A. Clifton, P. Green, H. Holttinen, L. Kitzing, B. Kosovic, J. K. Lundquist, J. Meyers, M. O'Malley, W. J. Shaw, and B. Straw, "Grand challenges: wind energy research needs for a global energy transition," *Wind Energy Science*, vol. 7, no. 6, pp. 2491–2496, 2022.

[7] G. V. Iungo, C. Santoni-Ortiz, M. Abkar, F. Porté-Agel, M. A. Rotea, and S. Leonardi, "Data-driven reduced order model for prediction of wind turbine wakes," *Journal of Physics: Conference Series*, vol. 625, p. 012009, jun 2015.

[8] J. Annoni, P. Gebraad, and P. Seiler, "Wind farm flow modeling using an input-output reduced-order model," in *2016 American Control Conference (ACC)*, 2016, pp. 506–512.

[9] N. Cassamo and J. W. van Wingerden, "On the potential of reduced order models for wind farm control: A koopman dynamic mode decomposition approach," *Energies*, vol. 13, no. 24, 2020.

[10] J. Meyers, C. Bottasso, K. Dykes, P. Fleming, P. Gebraad, G. Giebel, T. Göçmen, and J. W. Van Wingerden, "Wind farm flow control: prospects and challenges," *Wind Energy Science*, vol. 7, no. 6, pp. 2271–2306, 2022.

[11] W. Munters and J. Meyers, "Towards practical dynamic induction control of wind farms: analysis of optimally controlled wind-farm boundary layers and sinusoidal induction control of first-row turbines," *Wind Energy Science*, 02 2018.

[12] J. A. Frederik, B. M. Doekemeijer, S. P. Mulders, and J. W. van Wingerden, "The helix approach: Using dynamic individual pitch control to enhance wake mixing in wind farms," *Wind Energy*, vol. 23, no. 8, pp. 1739–1751, Aug. 2020.

[13] E. Taschner, A. A. W. van Vondelen, R. Verzijlbergh, and J. W. van Wingerden, "On the performance of the helix wind farm control approach in the conventionally neutral atmospheric boundary layer," *WAKE Conference 2023*.

[14] C. Muscari, P. Schito, A. Viré, A. Zasso, D. van der Hoek, and J. W. van Wingerden, "Physics informed DMD for periodic dynamic induction control of wind farms," *Journal of Physics: Conference Series*, vol. 2265, no. 2, p. 022057, may 2022.

[15] J. N. Kutz, S. L. Brunton, B. W. Brunton, and J. L. Proctor, *Dynamic Mode Decomposition: Data-Driven Modeling of Complex Systems*. Philadelphia, PA: Society for Industrial and Applied Mathematics, Nov. 2016.

[16] P. J. Baddoo, B. Herrmann, B. J. McKeon, J. N. Kutz, and S. L. Brunton, "Physics-informed dynamic mode decomposition (piDMD)," *arXiv:2112.04307 [physics]*, Dec. 2021, arXiv: 2112.04307.

[17] M. Churchfield, S. Lee, and P. Moriarty, "Overview of the simulator for wind farm application (SOWFA)," https://www.nrel.gov/wind/nwtc/assets/pdfs/sowfa-tutorial.pdf.